Inorganic Chemistry

Article

pubs.acs.org/IC

New Quaternary Rare-Earth Chalcogenides Ba*Ln*Sn_2Q_6 (*Ln* = Ce, Pr, Nd, Q = S; *Ln* = Ce, Q = Se): Synthesis, Structure, and Magnetic Properties

Kai Feng,[†,‡,§] Xu Zhang,[⊥,§] Wenlong Yin,[†,‡,§] Youguo Shi,[⊥] Jiyong Yao,*[,†,‡] and Yicheng Wu[†,‡]

[†]Center for Crystal Research and Development, Technical Institute of Physics and Chemistry, Chinese Academy of Sciences, Beijing 100190, China

[‡]Key Laboratory of Functional Crystals and Laser Technology, Technical Institute of Physics and Chemistry, Chinese Academy of Sciences, Beijing 100190, China

[§]University of the Chinese Academy of Sciences, Beijing 100049, China

[⊥]Beijing National Laboratory for Condensed Matter Physics, Institute of Physics, Chinese Academy of Sciences, Beijing 100190, China

Supporting Information

ABSTRACT: The first series of rare-earth chalcogenides with mixed-valence Sn atoms, namely the Ba*Ln*Sn_2Q_6 (*Ln* = Ce, Pr, Nd, Q = S; *Ln* = Ce, Q = Se) compounds, were synthesized via stoichiometric solid-state reactions at 1100 °C. Ba*Ln*Sn_2Q_6 belong to the polar space group $Pmc2_1$ of the orthorhombic system and contain mixed valent Sn atom in the ratio of Sn^{2+}/Sn^{4+} = 1:3. In the structure, the $Sn^{2+}Q_5$ rectangular pyramids, $Sn^{4+}Q_5$ trigonal bipyramids, $Sn^{4+}Q_6$ octahedra, and LnQ_8 bicapped trigonal prisms are connected with each other to form a three-dimensional framework with interspaces occupied by Ba^{2+} cations. As deduced from magnetic susceptibility measurements, $BaPrSn_2S_6$ and $BaNdSn_2S_6$ are paramagnetic and obey the Curie–Weiss law.

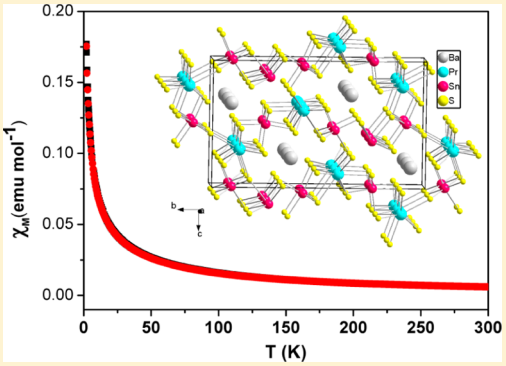

INTRODUCTION

Rare-earth chalcogenides have exhibited not only rich structures resulting from the diverse geometry of the *Ln*-centered coordination polyhedra and the flexible connectivity among them, but also fascinating magnetic, transport, and optical properties related to the 4f electrons.[1,2] Recently, rare-earth chalcogenides that also contain the p-block main group elements have received increasing attention.[3−37] Among them, $Na_{1.515}EuGeS_4$ contains a three-dimensional (3D) framework structure with empty nanotubules constructed by mixed valence Eu (II/III) cations;[33] $K_2Ln_2As_2Se_9$ (*Ln* = Sm, Gd)[38] is the first series of quaternary rare-earth selenoarsenate compounds with a 3D framework containing chairlike As_2Se_4 units; $ZnY_6Si_2S_{14}$,[25] Y_3GaS_6,[39] $La_2Ga_2GeS_8$,[29] $Eu_2Ga_2GeS_7$,[29] La_4GaSbS_9,[28] and Ba_2YInS_5[35] show strong second-harmonic generation (SHG) responses in the middle IR. In earlier studies, we carried out systematic investigation in the quaternary A/M/*Ln*/Q (A = alkaline-earth metal; M = group IIIA metals Ga or In; *Ln* = rare-earth element; Q = chalcogen) system, hoping that the introduction of alkaline-earth metal would help to increase the band gap and hence to increase the laser damage threshold for IR nonlinear optical (NLO) materials and avoid the two-photon absorption of the conventional 1 μm pumping source. As a result, a number of new compounds with the stoichiometry of Ba_2LnMQ_5 (M = Ga, In; *Ln* = rare-earth, Q = S, Se, Te)[35,36,40] and Ba_3LnInS_6[34] were obtained. They show four completely different structures and interesting magnetic properties. Furthermore, Ba_2YInQ_5 (Q = Se, Te) exhibit strong SHG response.[35]

So far, the p-block elements incorporated into the rare-earth chalcogenides are mainly the Group IIIA elements and the Group VA elements, while the study involving the Group IVA elements is very limited.[11,12,29,32,33,38,41−45] However, in view of the oxidation state and the coordination environment, the Group IVA elements, especially Ge and Sn, are unique among the p-block elements. Most of the p-block elements have only one stable oxidation state in chalcogenides: +1 for Tl; +2 for Pb; +3 for Al, Ga, In; +4 for Si; +5 for P; and +3 for As, Sb, Bi. Among them, Al^{3+}, Ga^{3+}, In^{3+}, Si^{4+}, and P^{5+} usually adopt the tetrahedral environment and Tl^{+}, Pb^{2+}, As^{3+}, Sb^{3+}, Bi^{3+} possess lone pair electrons. (Although the M–M bonding is possible for some p-block elements, which might affect the assignment of the formal oxidation states, it will not change the electronic configuration and coordination geometry.) In comparison, Ge and Sn can be stabilized in both the +2 oxidation state with

Received: November 26, 2013
Published: February 5, 2014

   dx.doi.org/10.1021/ic402934m | *Inorg. Chem.* 2014, 53, 2248−2253

electron lone pair and the +4 oxidation state typically in a tetrahedral environment, as shown by a number of compounds ranging from binary to quaternary ones such as MQ (M = Ge, Sn; Q = S, Se),[46−49] MQ_2 (M = Ge, Sn; Q = S, Se),[50−53] $Ba_7Sn_5S_{15}$,[54] $Ba_6Sn_6Se_{13}$,[55] Ba_2SnSe_5,[56−58] $Sr_4Sn_2Se_9$,[59] $La_2Ga_2GeS_8$,[29] $K_2FeGe_3Se_8$,[60] and $A_2Hg_3M_2S_8$ (A = K, Rb; M = Ge, Sn).[61] Such mixed valence property of Ge and Sn will increase the diversity in the stoichiometries and structures and may also lead to compounds with interesting properties. Here, in the search of new multinary rare earth chalcogenides, we focus on the Group IVA elements as the involved p-block elements and systematically investigate the quaternary A/M/*Ln*/Q (A = alkaline-earth metal; M = Group IVA elements Ge, Sn; *Ln* = rare-earth; Q = chalcogen) system. So far, two series of compounds were reported in this system, namely, the $MgLn_6Ge_2S_{14}$ series of compounds[62,63] and the $Eu_5Zr_3S_{12}$-related $Sr_2Y_{2.67}Sn_3S_{12}$, $Ca_3La_2Sn_3S_{12}$, and $Ca_3Er_2Sn_3S_{12}$ compounds,[45] in which the Group IVA elements Ge and Sn are all in the 4+ oxidation valence state. In this Paper, four new compounds $BaLnSn_2Q_6$ (*Ln* = Ce, Pr, Nd, Q = S; *Ln* = Ce, Q = Se) with mixed valent Sn were obtained. They possess the same structure composed of 3D frameworks with Ba atoms occupying the channels. $BaPrSn_2S_6$ and $BaNdSn_2S_6$ are paramagnetic and obey the Curie−Weiss law.

EXPERIMENTAL SECTION

Syntheses. Ba (99.9%), BaS (99%), Sn (99.9%), Se (99.9%), and S (99.99%), purchased from the Sinopharm Chemical Reagent Co., Ltd., and *Ln* (*Ln* = Ce, Pr, Nd) (99.9%), purchased from Alfa Aesar China (Tianjin) Co., Ltd., were used as received. The binary starting materials BaSe, SnS_2, and $SnSe_2$ were prepared from the direct reactions of the elements at high temperatures in sealed silica tubes evacuated to 10^{-3} Pa.

Crystal Growth of $BaLnSn_2Q_6$ (*Ln* = Ce, Pr, Nd, Q = S; *Ln* = Ce, Q = Se). The mixtures of BaQ (1 mmol), SnQ_2 (2 mmol), *Ln* (*Ln* = Ce, Pr, Nd, 1 mmol), and Q (1 mmol) were ground and loaded into fused-silica tubes under an Ar atmosphere in a glovebox. The tubes were flame-sealed under a high vacuum of 10^{-3} Pa and then placed in computer-controlled furnaces. They were heated to 1323 K in 24 h, left for 48 h, cooled to 693 K at a rate of 3 K/h, and finally cooled to room temperature by switching off the furnace. Dark red air-stable crystals were found.

The chip-shaped crystals were manually selected for structure characterization and determined as $BaLnSn_2Q_6$ (*Ln* = Ce, Pr, Nd, Q = S; *Ln* = Ce, Q = Se). Analyses of the crystals with an EDX-equipped Hitachi S-4800 SEM showed the presence of Ba, *Ln*, Sn, and Q in the approximate ratio of 1:1:2:6.

Structure Determination. The single-crystal X-ray diffraction measurements were performed on a Rigaku AFC10 diffractometer equipped with a graphite-monochromated Kα (λ = 0.71073 Å) radiation. The Crystalclear software[64] was used for data extraction and integration, and the program XPREP[65] was used for face-indexed absorption corrections.

The structures were solved with Direct Methods implemented in the program SHELXS and refined with the least-squares program SHELXL of the SHELXTL.PC suite of programs.[65] The final refinements of all structures include anisotropic displacement parameters and secondary extinction correction. The program STRUCTURE TIDY[66] was then employed to standardize the atomic coordinates. In addition, $BaCeSn_2S_6$ and $BaNdSn_2S_6$ were refined as racemic twins. Additional experimental details are given in Table 1, and selected metrical data are given in Table 2. Further information may be found in the Supporting Information.

Table 1. Crystal Data and Structure Refinements for $BaLnSn_2S_6$ (*Ln* = Ce, Pr, Nd) and $BaCeSn_2Se_6$

	$BaCeSn_2S_6$	$BaPrSn_2S_6$	$BaNdSn_2S_6$	$BaCeSn_2Se_6$
fw	707.20	707.99	711.32	988.60
space group	$Pmc2_1$	$Pmc2_1$	$Pmc2_1$	$Pmc2_1$
a (Å)	4.0665(8)	4.0478(2)	4.0098(8)	4.1908(8)
b (Å)	19.859(4)	19.8914(7)	19.761(4)	20.749(4)
c (Å)	11.873(2)	11.9303(5)	11.841(2)	12.406(3)
V (Å^3)	958.8(3)	960.58(7)	938.2(3)	1078.7(4)
ρ_c (g/cm^3)	4.899	4.896	5.036	6.087
μ (cm^{-1})	15.087	15.391	16.100	32.494
Flack parameter	0.09(5)	0.05(5)	0.24(3)	0.07(2)
$R(F)^a$	0.0424	0.0563	0.0280	0.0471
$R_W(F_o^2)^b$	0.0950	0.1448	0.0659	0.1039

$^aR(F) = \sum||F_o| - |F_c||/\sum|F_o|$ for $F_o^2 > 2\sigma(F_o^2)$. $^bR_w(F_o^2) = \{\sum[w(F_o^2 - F_c^2)^2]/\sum wF_o^4\}^{1/2}$ for all data. $w^{-1} = \sigma^2(F_o^2) + (z\,P)^2$, where $P = (\max(F_o^2, 0) + 2\,F_c^2)/3$.

Magnetic Susceptibility Measurements. Because of the low yields in our synthesis and the tiny size of the obtained

Table 2. Selected Interatomic Distances (Å) for $Ba_2LnSn_2S_6$ (*Ln* = Ce, Pr, Nd) and $BaCeSn_2Se_6$

	$BaCeSn_2S_6$	$BaPrSn_2S_6$	$BaNdSn_2S_6$	$BaCeSn_2Se_6$
Ba1−Q6 (× 2)	3.042(5)	3.104(7)	3.024(3)	3.191(2)
Ba1−Q5 (×2)	3.070(5)	3.142(6)	3.074(3)	3.221(2)
Ba1−Q7 (×2)	3.103(5)	3.167(7)	3.091(4)	3.246(2)
Ba1−Q1	3.267(7)	3.311(10)	3.252(5)	3.422(2)
Ba2−Q10 (×2)	3.267(5)	3.277(7)	3.249(3)	3.361(2)
Ba2−Q9 (×2)	3.286(5)	3.287(7)	3.277(3)	3.405(2)
Ba2−Q11 (×2)	3.297(5)	3.299(7)	3.289(3)	3.381(2)
Ba2−Q8 (×2)	3.305(5)	3.306(6)	3.299(3)	3.437(2)
Ln1−Q5 (×2)	2.929(5)	2.876(6)	2.880(3)	3.022(2)
Ln1−Q6 (×2)	3.004(5)	2.954(6)	2.966(3)	3.080(2)
Ln1−Q2	3.007(7)	3.005(10)	3.010(4)	3.139(2)
Ln1−Q8 (×2)	3.030(4)	3.023(6)	2.987(3)	3.148(2)
Ln1−Q1	3.039(7)	3.082(8)	3.018(5)	3.191(2)
Ln2−Q11 (×2)	2.935(4)	2.925(6)	2.903(3)	3.065(2)
Ln2−Q10 (×2)	2.941(4)	2.937(6)	2.902(3)	3.070(2)
Ln2−Q12 (×2)	2.944(4)	2.929(7)	2.910(3)	3.063(2)
Ln2−Q4	3.203(6)	3.183(8)	3.183(4)	3.323(2)
Ln2−Q3	3.265(7)	3.264(11)	3.233(4)	3.352(3)
Sn1−Q7 (×2)	2.907(4)	2.873(6)	2.874(3)	3.016(2)
Sn1−Q2	2.916(6)	2.912(9)	2.902(4)	3.031(2)
Sn1−Q9 (×2)	2.997(5)	2.993(6)	2.961(3)	3.108(2)
Sn2−Q7	2.619(7)	2.574(10)	2.586(5)	2.681(2)
Sn2−Q1 (×2)	2.629(4)	2.641(6)	2.622(3)	2.758(2)
Sn2−Q5	2.594(7)	2.581(9)	2.587(5)	2.694(2)
Sn2−Q2 (×2)	2.697(4)	2.682(6)	2.659(3)	2.781(2)
Sn3−Q8	2.425(6)	2.428(9)	2.417(4)	2.558(2)
Sn3−Q4 (×2)	2.476(4)	2.484(5)	2.468(3)	2.606(1)
Sn3−Q10	2.541(6)	2.529(8)	2.531(4)	2.691(2)
Sn3−Q6	2.551(6)	2.534(8)	2.540(4)	2.674(2)
Sn4−Q9	2.418(6)	2.410(8)	2.417(4)	2.556(2)
Sn4−Q3 (×2)	2.488(3)	2.480(5)	2.469(2)	2.610(1)
Sn4−Q11	2.530(6)	2.536(9)	2.518(4)	2.682(2)
Sn4−Q12	2.559(6)	2.575(10)	2.556(4)	2.701(2)

dx.doi.org/10.1021/ic402934m | Inorg. Chem. 2014, 53, 2248−2253

crystals, only enough $BaPrSn_2S_6$ and $BaNdSn_2S_6$ crystals can be picked for measuring magnetic susceptibility. A SQUID magnetometer (Quantum Design) operating at 10k Oe was used to carry out magnetic susceptibility measurements. Single crystals of $BaPrSn_2S_6$ and $BaNdSn_2S_6$ (about 10−20 mg) were ground and loaded into gelatin capsules placed on Cu pole for measurement of the magnetism. The background was deducted by SQUID system before measurement. The samples were gathered in a sample holder and cooled to the low-temperature limit. The magnetic field was then applied to the samples, then they were slowly warmed to 300 K (zero-field cooling, ZFC), followed by cooling in the field (field cooling, FC). The data were corrected for the diamagnetic susceptibility from the sample holder.

RESULTS AND DISCUSSION

Crystal Growth. Three sulfides $BaLnSn_2S_6$ (*Ln* = Ce, Pr, Nd) and one selenide $BaCeSn_2Se_5$ crystals have been obtained by spontaneous nucleation method for the first time. The yields range from 10% to 20% based on *Ln*. Great efforts have been made to synthesize analogues containing other rare-earth elements available to us, namely, Y, La, Sm, Gd, Dy, Er, and Lu for $BaLnSn_2S_6$ and Y, La, Ce, Pr, Nd, Gd, Dy, Er, Yb, and Lu for $BaCeSn_2Se_6$, which was not successful. Thus we only report the four members we obtained here.

Structure of $BaLnSn_2Q_6$ (*Ln* = Ce, Pr, Nd, Q = S; *Ln* = Ce, Q = Se). The four compounds, $BaLnSn_2S_6$ (*Ln* = Ce, Pr, Nd) and $BaCeSn_2Se_6$, are isotypic, so only the structure of $BaCeSn_2S_6$ will be discussed in detail here. As shown in Figure 1, $BaCeSn_2S_6$ crystallizes in the space group $Pmc2_1$ of the

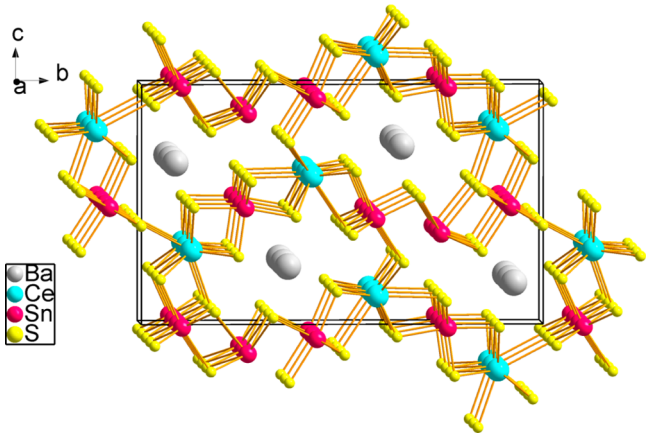

Figure 1. Crystal structure of $BaCeSn_2S_6$.

orthorhombic system with unit cell permanents of a = 4.067(1) Å, b = 19.859(4) Å, c = 11.873(2) Å, and Z = 4. The asymmetric unit of $BaCeSn_2S_6$ contains two crystallographically independent Ba atoms, two Ce atoms, four Sn atoms, and twelve S atoms, which are fully set on the Wyckoff positions 2*a* or 2*b* with no disordered atom occupancy.

Figure 2 displays the coordination environments of cations in $BaCeSn_2S_6$. The four Sn atoms have three kinds of coordination environments. Sn1 atom is coordinated to five S atoms with three short Sn1−S bonds ranging from 2.907(4) to 2.916(6) Å and two longer Sn1−S bonds of 2.997(5) Å. The calculated band valence sum (BVS)[67] is 1.75. Such bond lengths and BVS value resemble those of Sn^{2+} cation in other chalcogenides, including the binary SnS[49] (3.000 Å), ternary

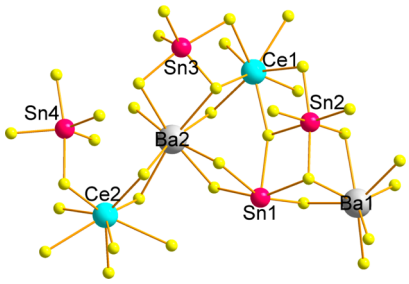

Figure 2. Coordination environments of all cations in $BaCeSn_2S_6$.

$Sn_{0.33}NbS_3$[68] (3.004(1) to 3.004(5) Å), and quaternary $TlSnPS_4$[69] (2.721 to 3.090(1) Å) and $Hg_2SnS_2Br_2$[70] (2.909(5) to 3.217(5) Å). Sn2 is enjoined to six S atoms to generate a distorted octahedron with Sn−S bond lengths from 2.594(7) to 2.697(4) Å, while both Sn3 and Sn4 atoms are surrounded by five S atoms in trigonal bipyramidal geometry with Sn−S bond lengths from 2.418(6) to 2.559(6) Å. The calculated BVSs of Sn3 and Sn4 are 3.90 and 3.87, respectively, which are close to the oxidation state 4+. However, the calculated BVS[67] of Sn2 is 3.11, smaller than the oxidation state 4+, but comparable with the 6-coordinated Sn^{4+} cation in $BaSnS_3$[71] (3.484). Moreover the Sn*N*−S (*N* = 2, 3, 4) bond lengths are consistent with those in compounds containing Sn^{4+} cations. For example, the Sn^{4+} cation is coordinated to six S atoms, with the bond length of 2.538(1) to 2.650(1) Å in $BaSnS_3$[71], and the Sn^{4+} cation is 5-coordinated, with the Sn−S bond length ranging from 2.421(4) to 2.596(3) Å in $BaSn_2S_5$.[54] As for the two Ce atoms, they are both linked to eight S atoms in bicapped trigonal prism geometry with Ce−S bond length varying from 2.929(5) to 3.265(7) Å, comparable to those in $BaCe_2FeS_5$[72] (2.791(1) to 3.095(1) Å) and $K_3CeP_2S_8$[73] (2.884(2) to 3.346(2) Å). In addition, the calculated BVS[67] values for the two Ce atoms are close to the expected value of +3. The Ba1 and Ba2 atoms are in 7 and 8-fold coordination environment with two kinds of coordination geometry: monocapped trigonal prism and distorted rectangular prism, respectively. The Ba−S distances lie in the range of 3.042(5) to 3.305(5) Å, which are common in Ba-containing sulfides such as Ba_2AgInS_4[74] (3.128(2) to 3.314(2) Å) and Ba_3PrInS_6[34] (3.171(1) to 3.335(1) Å). Considering the bonding and coordination environment in the structure, the oxidation state of 2+, 3+, 2+, 4+, and 2− can be assigned to Ba, Ce, Sn1, Sn*N* (*N* = 2, 3, 4), and S atoms, respectively, and the formula may be represented as $Ba_2^{2+}Ce_2^{3+}Sn^{2+}Sn_3^{4+}S_{12}^{2-}$.

The diverse coordination environments of Sn have great influence on the connectivity of atoms in the structure. As shown in Figure 3, the $Sn3Se_5$ trigonal bipyramid are

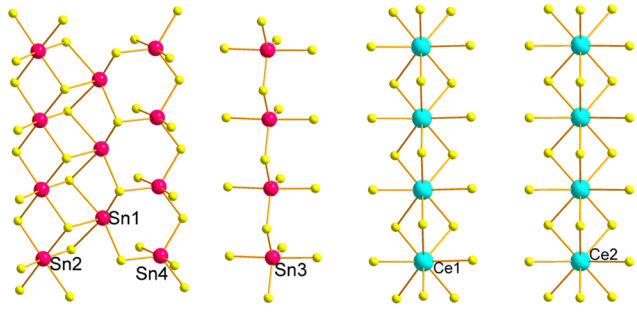

Figure 3. Structure of slab and chains in $BaCeSn_2S_6$.

dx.doi.org/10.1021/ic402934m | Inorg. Chem. 2014, 53, 2248−2253

interconnected with each other via corner-sharing S atoms to generate the one-dimensional (1D) chain of $^1_\infty[SnS_4]^{4-}$ spreading parallel to the crystallographic *a* direction. Similar chains are also formed for $Sn4S_5$, $Sn1S_5$, and $Sn2S_6$ polyhedra by corner-, edge- and edge-sharing S atoms, respectively. These chains are further linked in sequence of $Sn4S_5$, $Sn1S_5$, and $Sn2S_6$ to form the 1D slab of $^1_\infty[Sn^{2+}Sn^{4+}_2S_8]^{6-}$ extending parallel to the crystallographic *a* direction. The $Sn4S_5$ and $Sn1S_5$ chains are linked by corner-sharing S atoms, while the $Sn1S_5$ and $Sn2S_6$ chains are connected through sharing edges. Lastly, the slabs and chains are connected by the $^1_\infty[CeS_5]^{7-}$ chains, which are comprised of the CeS_8 bicapped trigonal prisms, to generate the 3D framework of $^3_\infty[LnSn_2Q_6]^{4-}$ with interspaces occupied by Ba^{2+} cations along *a* direction.

In the quaternary A/M/*Ln*/Q (A = alkaline-earth metal; M = Group IVA metal Ge, Sn; *Ln* = rare-earth; Q = chalcogen) system, two other series of compounds were reported, that is, the $MgLn_6Ge_2S_{14}$ series of compounds[62,63] and the $Eu_5Zr_3S_{12}$-related isotypic $Sr_2Y_{2.67}Sn_3S_{12}$, $Ca_3La_2Sn_3S_{12}$, and $Ca_3Er_2Sn_3S_{12}$ compounds.[45] In $MgLn_6Ge_2S_{14}$, all the Ge atoms are coordinated to four S atoms with the oxidation state of 4+, and the GeS_4 tetrahedra are isolated from each other. In $Ca_3La_2Sn_3S_{12}$, the Sn atoms are also in the 4+ oxidation state but are surrounded by an octahedron of six S atoms, and the SnS_6 octahedra are condensed into a chain via edge-sharing. In comparison, the Sn in $BaLnSn_2S_6$ are in mixed valences of 2+ and 4+, and the SnS_n (n = 5, 6) polyhedra are connected with each other to generate slabs and chains. As for the connectivity among the rare-earth atoms, there are also some obvious differences among the three types of structures: the CeS_8 bicapped trigonal prisms in $MgLn_6Ge_2S_{14}$ are connected with each other to form a 3D framework, with GeS_4 tetrahedra occupying the cave and MgS_6 octahedra (half occupancy) in the channels; the LaS_7 monocapped trigonal prisms in $Ca_3La_2Sn_3S_{12}$ form complex chains via edge-sharing, which are further connected by the chains of SnS_6 chains to generate the 3D framework; while the LnQ_8 bicapped trigonal prisms in $BaLnSn_2Q_6$ only form simple chains by themselves, which are then connected to chains of SnS_n (n = 5, 6) polyhedra to build a 3D framework, with Ba atoms occupying the channels.

Magnetic Susceptibility Measurement. The temperature variations of the molar magnetic susceptibility (χ_m) and the inverse magnetic susceptibility ($1/\chi_m$) for $BaPrSn_2S_6$ and $BaNdSn_2S_6$ are illustrated in Figure 4A,B. The ZFC magnetic susceptibility and the FC magnetic susceptibility data are essentially superimposable at all temperatures.

The magnetic susceptibility data of the $BaPrSn_2S_6$ and $BaNdSn_2S_6$ samples were fitted by a least-squares method to Curie–Weiss law: $\chi_m = C/(T - \theta)$, where C is the Curie constant, T is the absolute temperature, and θ is the Weiss constant. The effective magnetic moment (μ_{eff} (total)) was calculated from the equation μ_{eff} (total) = $(8C)^{1/2}\mu_B$.[75]

As shown, they both are paramagnetic and obey the Curie–Weiss law over the entire experimental temperature range. As deduced from the fitting results, the values of C and θ for $BaPrSn_2S_6$ and $BaNdSn_2S_6$ are 1.30 emu K mol^{-1}, −24.94 K and 1.92 emu K mol^{-1}, −17.64 K, respectively. The calculated effective magnetic moments are 3.92 μ_B/Pr atom and 3.22 μ_B/Nd atom, which are a little different from the calculated theoretical value for Pr^{3+} (3.58 μ_B/Pr atom) and Nd^{3+} ion (3.62 μ_B/Nd atom).[75] This may be due to tiny amount of impure phase, which is attached to the surfaces of the picked crystals and impossible to get rid of. In addition, the negative θ values

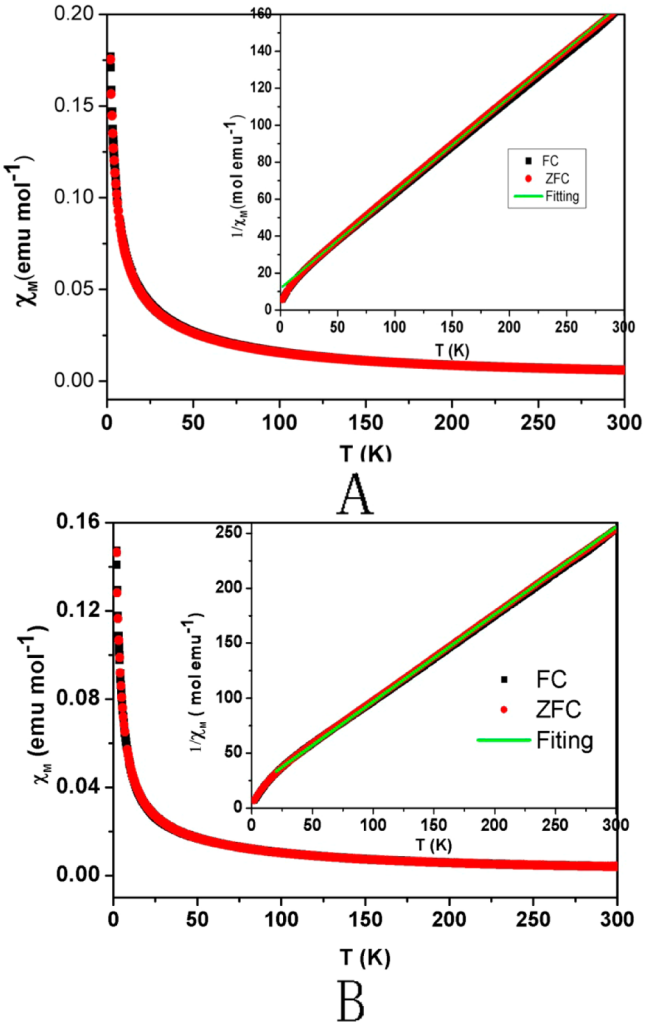

Figure 4. (**A**) χ_m vs temperature of $BaPrSn_2S_6$ for FC and ZFC data. Inset shows the plot of $1/\chi_m$ vs temperature. (**B**) χ_m vs temperature of $BaNdSn_2S_6$ for FC and ZFC data. Inset shows the plot of $1/\chi_m$ vs temperature.

may suggest weak short-range antiferromagnetic interaction among the adjacent Ln^{3+} cations. The distances between the nearest $Pr^{3+}\cdots Pr^{3+}$ and $Nd^{3+}\cdots Nd^{3+}$ cations are 4.048(1) and 4.010(1) Å along *a* direction, which may induce certain interaction between Ln^{3+} cations.

CONCLUSIONS

In summary, four new rare-earth chalcogenides in the quaternary Ba/*Ln*/M/Q (*Ln* = rare-earth; M = Group IVA element; Q = chalcogen) system, namely, the $BaLnSn_2S_6$ (*Ln* = Ce, Pr, Nd) and $BaCeSn_2Se_6$ compounds, have been obtained and characterized. They represent the first series of rare-earth chalcogenides with mixed-valence Sn atoms. $BaLnSn_2Q_6$ crystallize in the polar space group $Pmc2_1$ of the orthorhombic system and possess both Sn^{2+} and Sn^{4+} atoms in three kinds of conformation. The structure features infinite 3D anionic framework $^3_\infty[LnSn_2Q_6]^{4-}$, consisting of alternate $^1_\infty[SnQ_4]^{4-}$, $^1_\infty[Sn^{2+}Sn^{4+}_2Q_8]^{6-}$, and $^1_\infty[CeQ_5]^{7-}$ chains, with interspaces located by Ba atoms. Magnetic property measurement demonstrates that $BaPrSn_2S_6$ and $BaNdSn_2S_6$ exhibit paramagnetic behavior, obeying the Curie–Weiss law to 2 K.

dx.doi.org/10.1021/ic402934m | Inorg. Chem. 2014, 53, 2248–2253

■ ASSOCIATED CONTENT

Supporting Information

Crystallographic file in CIF format for $BaLnSn_2S_6$ (*Ln* = Ce, Pr, Nd) and $BaCeSn_2Se_6$. This material is available free of charge via the Internet at http://pubs.acs.org.

■ AUTHOR INFORMATION

Corresponding Author

*E-mail: jyao@mail.ipc.ac.cn.

Notes

The authors declare no competing financial interest.

■ ACKNOWLEDGMENTS

This research was supported by the National Basic Research Project of China (No. 2010CB630701), National Natural Science Foundation of China (No. 91122034, No. 21271178), and the Ministry of Science and Technology of China (973 Project No. 2011CBA00110).

■ REFERENCES

(1) Flahaut, J. In *Handbook on the Physics and Chemistry of Rare Earths;* Karl A. Gschneidner, Jr., LeRoy, E., Eds.; Elsevier: 1979; Vol. *4*, p 1−88.

(2) Cotton, S. *Lanthanide and Actinides;* Oxford University Press: New York, 1991.

(3) Carpenter, J. D.; Hwu, S. J. *Chem. Mater.* **1992**, *4*, 1368−1372.

(4) Bucher, C. K.; Hwu, S. J. *Inorg. Chem.* **1994**, *33*, 5831−5835.

(5) Sutorik, A. C.; Albrittonthomas, J.; Kannewurf, C. R.; Kanatzidis, M. G. *J. Am. Chem. Soc.* **1994**, *116*, 7706−7713.

(6) Carpenter, J. D.; Hwu, S. J. *Inorg. Chem.* **1995**, *34*, 4647−4651.

(7) Sutorik, A. C.; AlbrittonThomas, J.; Hogan, T.; Kannewurf, C. R.; Kanatzidis, M. G. *Chem. Mater.* **1996**, *8*, 751−761.

(8) Patschke, R.; Brazis, P.; Kannewurf, C. R.; Kanatzidis, M. *Inorg. Chem.* **1998**, *37*, 6562−6563.

(9) Patschke, R.; Heising, J.; Kanatzidis, M.; Brazis, P.; Kannewurf, C. R. *Chem. Mater.* **1998**, *10*, 695−697.

(10) Huang, F. Q.; Ibers, J. A. *Inorg. Chem.* **1999**, *38*, 5978−5983.

(11) Aitken, J. A.; Larson, P.; Mahanti, S. D.; Kanatzidis, M. G. *Chem. Mater.* **2001**, *13*, 4714−4721.

(12) Evenson, C. R.; Dorhout, P. K. *Inorg. Chem.* **2001**, *40*, 2409−2414.

(13) Huang, F. Q.; Mitchell, K.; Ibers, J. A. *Inorg. Chem.* **2001**, *40*, 5123−5126.

(14) Mitchell, K.; Haynes, C. L.; McFarland, A. D.; Van Duyne, R. P.; Ibers, J. A. *Inorg. Chem.* **2002**, *41*, 1199−1204.

(15) Mitchell, K.; Ibers, J. A. *Chem. Rev.* **2002**, *102*, 1929−1952.

(16) Mitchell, K.; Huang, F. Q.; McFarland, A. D.; Haynes, C. L.; Somers, R. C.; Van Duyne, R. P.; Ibers, J. A. *Inorg. Chem.* **2003**, *42*, 4109−4116.

(17) Mitchell, K.; Huang, F. Q.; Caspi, E. N.; McFarland, A. D.; Haynes, C. L.; Somers, R. C.; Jorgensen, J. D.; Van Duyne, R. P.; Ibers, J. A. *Inorg. Chem.* **2004**, *43*, 1082−1089.

(18) Wakeshima, M.; Furuuchi, F.; Hinatsu, Y. *J. Phys.: Condens. Matter* **2004**, *16*, 5503−5518.

(19) Yao, J. Y.; Deng, B.; Sherry, L. J.; McFarland, A. D.; Ellis, D. E.; Van Duyne, R. P.; Ibers, J. A. *Inorg. Chem.* **2004**, *43*, 7735−7740.

(20) Zeng, H.-Y.; Mattausch, H.; Simon, A.; Zheng, F.-K.; Dong, Z.-C.; Guo, G.-C.; Huang, J.-S. *Inorg. Chem.* **2006**, *45*, 7943−7946.

(21) Chan, G. H.; Sherry, L. J.; Van Duyne, R. P.; Ibers, J. A. *Z. Anorg. Allg. Chem.* **2007**, *633*, 1343−1348.

(22) Chan, G. H.; Lee, C.; Dai, D.; Whangbo, M.-H.; Ibers, J. A. *Inorg. Chem.* **2008**, *47*, 1687−1692.

(23) Choudhury, A.; Dorhout, P. K. *Inorg. Chem.* **2008**, *47*, 3603−3609.

(24) Liu, Y.; Chen, L.; Wu, L.-M. *Inorg. Chem.* **2008**, *47*, 855−862.

(25) Guo, S.-P.; Guo, G.-C.; Wang, M.-S.; Zou, J.-P.; Xu, G.; Wang, G.-J.; Long, X.-F.; Huang, J.-S. *Inorg. Chem.* **2009**, *48*, 7059−7065.

(26) Zhao, H.-J.; Li, L.-H.; Wu, L.-M.; Chen, L. *Inorg. Chem.* **2009**, *48*, 11518−11524.

(27) Zhao, H.-J.; Li, L.-H.; Wu, L.-M.; Chen, L. *Inorg. Chem.* **2010**, *49*, 5811−5817.

(28) Chen, M.-C.; Li, L.-H.; Chen, Y.-B.; Chen, L. *J. Am. Chem. Soc.* **2011**, *133*, 4617−4624.

(29) Chen, M.-C.; Li, P.; Zhou, L.-J.; Li, L.-H.; Chen, L. *Inorg. Chem.* **2011**, *50*, 12402−12404.

(30) Jin, G. B.; Choi, E. S.; Guertin, R. P.; Booth, C. H.; Albrecht-Schmitt, T. E. *Chem. Mater.* **2011**, *23*, 1306−1314.

(31) Meng, C.-Y.; Chen, H.; Wang, P.; Chen, L. *Chem. Mater.* **2011**, *23*, 4910−4919.

(32) Bera, T. K.; Kanatzidis, M. G. *Inorg. Chem.* **2012**, *51*, 4293−4299.

(33) Choudhury, A.; Grandjean, F.; Long, G. J.; Dorhout, P. K. *Inorg. Chem.* **2012**, *51*, 11779−11786.

(34) Feng, K.; Shi, Y.; Yin, W.; Wang, W.; Yao, J.; Wu, Y. *Inorg. Chem.* **2012**, *51*, 11144−11149.

(35) Yin, W.; Feng, K.; Wang, W.; Shi, Y.; Hao, W.; Yao, J.; Wu, Y. *Inorg. Chem.* **2012**, *51*, 6860−6867.

(36) Yin, W.; Wang, W.; Bai, L.; Feng, K.; Shi, Y.; Hao, W.; Yao, J.; Wu, Y. *Inorg. Chem.* **2012**, *51*, 11736−11744.

(37) Zhao, H.-J.; Zhang, Y.-F.; Chen, L. *J. Am. Chem. Soc.* **2012**, *134*, 1993−1995.

(38) Wu, Y.; Bensch, W. *Inorg. Chem.* **2009**, *48*, 2729−2731.

(39) Zhang, M.-J.; Li, B.-X.; Liu, B.-W.; Fan, Y.-H.; Li, X.-G.; Zeng, H.-Y.; Guo, G.-C. *Dalton Trans.* **2013**, *42*, 14223−14229.

(40) Feng, K.; Yin, W.; Wang, W.; Kang, L.; Hao, W.; Yao, J.; Shi, Y.; Lin, Z.; Wu, Y. *Z. Anorg. Allg. Chem.* **2013**, *639*, 1021−1025.

(41) Klawitter, Y.; Bensch, W.; Wickleder, C. *Chem. Mater.* **2005**, *18*, 187−197.

(42) Wu, Y.; Näther, C.; Bensch, W. *Inorg. Chem.* **2006**, *45*, 8835−8837.

(43) Bera, T. K.; Kanatzidis, M. G. *Inorg. Chem.* **2008**, *47*, 7068−7070.

(44) Assoud, A.; Kleinke, H. *Solid State Sci.* **2010**, *12*, 919−923.

(45) Zeng, H.-Y.; Zhao, Z.-Y.; Guo, S.-P.; Zheng, F.-K.; Guo, G.-C.; Huang, J.-S. *J. Alloys Compd.* **2012**, *514*, 135−140.

(46) Zachariasen, W. H. *Phys. Rev.* **1932**, *40*, 0917−0922.

(47) Okazaki, A. *J. Phys. Soc. Jpn.* **1958**, *13*, 1151−1155.

(48) Adouby, K.; Perez-Vicente, C.; Jumas, J. C.; Fourcade, R.; Toure, A. A. *Z. Kristallogr.* **1998**, *213*, 343−349.

(49) Slipukhina, I. V.; Bercha, D. M. *Phys. Status Solidi B* **2007**, *244*, 650−668.

(50) Dittmar, G.; Schafer, H. *Acta Crystallogr., Sect. B: Struct. Sci.* **1976**, *32*, 1188−1192.

(51) Alalamy, F. A. S.; Balchin, A. A.; White, M. *J. Mater. Chem. Sci.* **1977**, *12*, 2037−2042.

(52) Palosz, B.; Salje, E. *J. Appl. Crystallogr.* **1989**, *22*, 622−623.

(53) Grande, T.; Ishii, M.; Akaishi, M.; Aasland, S.; Fjellvag, H.; Stolen, S. *J. Solid State Chem.* **1999**, *145*, 167−173.

(54) Luo, Z.-Z.; Lin, C.-S.; Cheng, W.-D.; Zhang, H.; Zhang, W.-L.; He, Z.-Z. *Inorg. Chem.* **2013**, *52*, 273−279.

(55) Feng, K.; Jiang, X.; Kang, L.; Yin, W.; Hao, W.; Lin, Z.; Yao, J.; Wu, Y.; Chen, C. *Dalton Trans.* **2013**, *42*, 13635−13641.

(56) Assoud, A.; Soheilnia, N.; Kleinke, H. *J. Solid State Chem.* **2005**, *178*, 1087−1093.

(57) Graf, C.; Assoud, A.; Zelinska, M.; Kleinke, H. *Z. Anorg. Allg. Chem.* **2010**, *636*, 1821−1826.

(58) Zelinska, M.; Assoud, A.; Graf, C.; Kleinke, H. *Inorg. Chem.* **2010**, *49*, 1090−1093.

(59) Pocha, R.; Johrendt, D. *Inorg. Chem.* **2004**, *43*, 6830−6837.

(60) Feng, K.; Wang, W.; He, R.; Kang, L.; Yin, W.; Lin, Z.; Yao, J.; Shi, Y.; Wu, Y. *Inorg. Chem.* **2013**, *52*, 2022−2028.

(61) Liao, J. H.; Marking, G. M.; Hsu, K. F.; Matsushita, Y.; Ewbank, M. D.; Borwick, R.; Cunningham, P.; Rosker, M. J.; Kanatzidis, M. G. *J. Am. Chem. Soc.* **2003**, *125*, 9484−9493.

(62) Gitzendanner, R. L.; Spencer, C. M.; DiSalvo, F. J.; Pell, M. A.; Ibers, J. A. *J. Solid State Chem.* **1997**, *131*, 399−404.
(63) Huch, M. R.; Gulay, L. D.; Ekseyuk, I. D. *J. Alloys Compd.* **2006**, *424*, 114−118.
(64) Rigaku *CrystalClear;* Rigaku Corporation: Tokyo, Japan, 2008.
(65) Sheldrick, G. M. *Acta Crystallogr., Sect. A: Found. Crystallogr.* **2008**, *64*, 112−122.
(66) Gelato, L. M.; Parthe, E. *J. Appl. Crystallogr.* **1987**, *20*, 139−143.
(67) Brown, I. D.; Altermatt, D. *Acta Crystallogr., Sect. B: Struct. Sci.* **1985**, *41*, 244−247.
(68) Fang, C. M.; Wiegers, G. A.; Meetsma, A.; deGroot, R. A.; Haas, C. *Phys. B* **1996**, *226*, 259−267.
(69) Becker, R.; Brockner, W.; Eisenmann, B. *Z. Naturforsch., A: Phys. Sci.* **1987**, *42*, 1309−1312.
(70) Blachnik, R.; Lytze, K.; Reuter, H. *J. Solid State Chem.* **1996**, *126*, 95−98.
(71) Yamaoka, S.; Okai, B. *Mater. Res. Bull.* **1970**, *5*, 789−793.
(72) Ino, K.; Wakeshima, M.; Hinatsu, Y. *Mater. Res. Bull.* **2001**, *36*, 2207−2213.
(73) Gauthier, G.; Jobic, S.; Brec, R.; Rouxel, J. *Inorg. Chem.* **1998**, *37*, 2332−2333.
(74) Yin, W.; Feng, K.; Mei, D.; Yao, J.; Fu, P.; Wu, Y. *Dalton Trans.* **2012**, *41*, 2272−2276.
(75) O'Connor, C. J. Magnetochemistry—Advances in Theory and Experimentation. In *Progress in Inorganic Chemistry;* Lippard, S. J., Ed.; John Wiley & Sons, Inc.: New York, 2007; Vol. *29*, pp 203−283.